The definitive version of this article is published as:
Morozov, M., Tian, G.Y., Edgar, D. Comparison of PEC and SFEC NDE techniques, *Nondestructive Testing and Evaluation*, Volume 24, Issue 1-2, March 2009, Pages 153-164
http://www.informaworld.com/openurl?genre=article&issn=1058-9759&volume=24&issue=1&spage=153

Comparison of PEC and SFEC NDE Techniques

Maxim Morozov[a*], Gui Yun Tian[a] and David Edgar[b]

[a]*School of Electrical, Electronic and Computing Engineering, Newcastle University, Merz Court, Newcastle upon Tyne, NE1 7RU, United Kingdom;* [b]*NDE Group, QinetiQ, Cody Technology Park, Farnborough, Hampshire, GU14 0LX, United Kingdom*

_____

*Corresponding author. Email: maxim.morozov@ncl.ac.uk

Abstract: Eddy current testing is one of the most widely used non-destructive evaluation (NDE) techniques. The recent development of multiple frequency and pulsed eddy current (PEC) NDE has demonstrated high potential for applications in quantitative NDE in terms of defect profiles, defect depths and 3D defect reconstruction in particular. This paper systematically investigates eddy current behaviour in the frequency domain. Two methods, Swept Frequency Eddy Current (SFEC) and Pulsed Eddy Current are comparatively studied with respect to their capability to discriminate among various test cases. It is demonstrated that using PEC we can discriminate between the upper and reverse surface slots, as well as various sample thicknesses, with resolution compatible to SFEC in a single excitation cycle.

Keywords*:* non-destructive evaluation; pulsed eddy currents; swept frequency eddy currents; frequency domain.

1. Introduction

Non-Destructive Evaluation (NDE) plays a critical role in the maintenance of engineering components and structures. As its outcome, an NDE process enables monitoring of the intactness of structural components and indicates the eventual need for repairs. Electromagnetic NDE by means of Eddy Current (EC) offers various advantages compared to other principal NDE techniques: it enables detection of subsurface defects, as well as surface ones, in contrast to dye penetrant inspection; it can be applied to non-magnetic conductive test pieces in contrast to magnetic particles inspection; it does not require an acoustic couplant as ultrasonic inspection does and it is more economical and less hazardous than radiography. EC testing is based on the principle of electromagnetic induction where a time-alternating magnetic field of a coil induces electric (eddy) currents in an electrically conductive test piece brought into the proximity of the coil. The secondary magnetic field of the induced eddy currents impedes propagation of the external electro-magnetic field into a test piece and the standard depth of penetration δ, defined as the depth at which the current density has exponentially decayed to 1/e of the value at the surface, is given by equation 1 when the plane wave, i.e. low spatial frequency, assumption is made for the excitation field [1, 2].

$$\delta = \sqrt{\frac{2}{\omega\sigma\mu}}, \tag{1}$$

where $\omega = 2\pi f$ is the angular frequency of excitation, σ is the conductivity of the sample and μ is the magnetic permeability of the material under examination.

This phenomenon is known as the skin effect. Hence application of different frequencies is needed to examine thick test pieces for both the surface and sub-surface conditions. Analysis of EC signals in the frequency domain helps to enhance test-piece characterisation by providing an additional dimension of information to traditional phasor measurements at a single excitation frequency. It can be easily performed using an impedance analyser in swept frequency mode [3-7]. This approach, called Swept Frequency Eddy Current (SFEC) inspection, offers a high precision and broad bandwidth. However, for higher spectral resolution and accuracy requirements, the sweep duration is longer, leading to lengthy inspection times. A solution to this problem might be multi-frequency (MUF) EC when the excitation signal contains several frequency components [8]. Implementation of such an excitation becomes increasingly sophisticated with a growing number of desired frequencies. The pulsed EC (PEC) technique, where the coil is driven with a rectangular current waveform, offers an answer to the broad-band excitation challenge. The PEC response contains frequency-rich information and shows promising results in detecting flaws at greater depths [9]. The PEC technique is predominantly a time domain method. Several time-domain features, namely the time to peak, the peak height and more recently reported rising point and zero crossing of the PEC signal are used in PEC testing to identify and characterise defects in metallic targets [10, 11]. Advanced signal analysis approaches are needed in order to extract test case related features from a time domain PEC signal, for instance principal component analysis for PEC [12]. Hence there have been efforts to facilitate PEC response interpretation by frequency domain analysis [13, 14].

In this work we investigate the correlation between frequency domain signals obtained by PEC and SFEC techniques. Dependencies of the SFEC and PEC responses on various test cases are presented and compared. Correlation of the frequency domain PEC response with the better understood SFEC method is aimed at implementing an efficient test piece characterisation by the much faster PEC method.

2. Experimental setup and samples

Two test sample cases have been examined:

1. Sample with steps of various thickness from 1 mm to 10 mm with increment of 1 mm, shown in Fig.1.

2. Sample with 3 mm wide slots of various depth (3, 5, 7 and 9 mm) shown in Fig.2. The slots have been tested both on the surface they originate from and the reverse surface and will be referred to as inner defects (ID) and outer defects (OD) respectively.

The samples represent 10 mm thick slabs and are made from aluminium with electrical conductivity 26.6 MS/m.

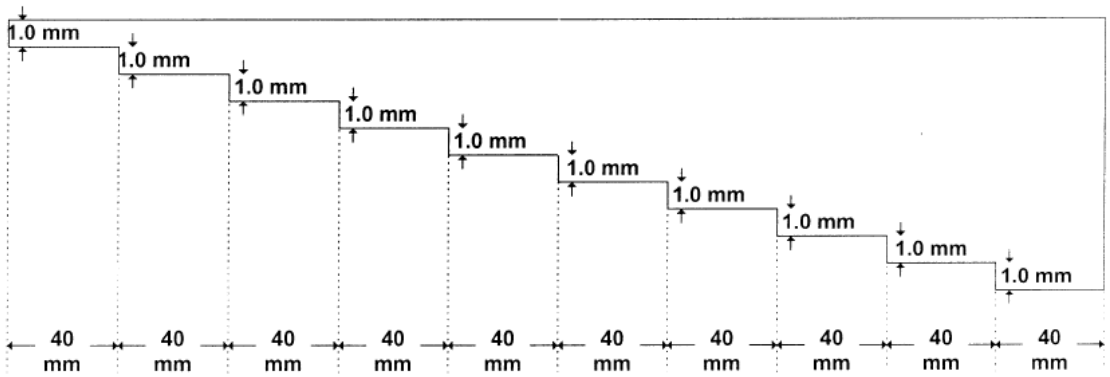

Figure 1. Step sample (no. 1) profile.

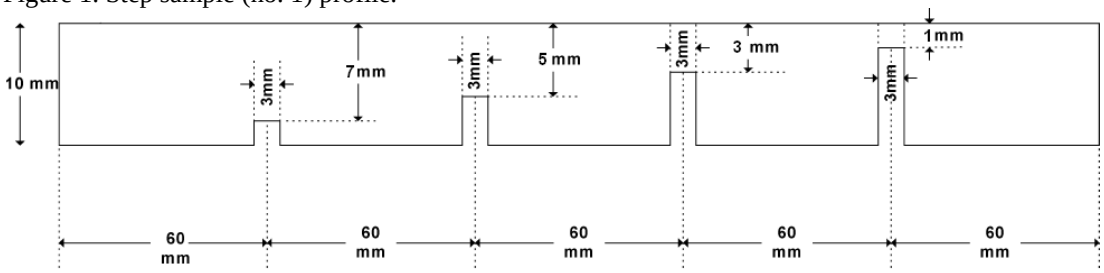

Figure 2. Slot sample (no. 2) profile.

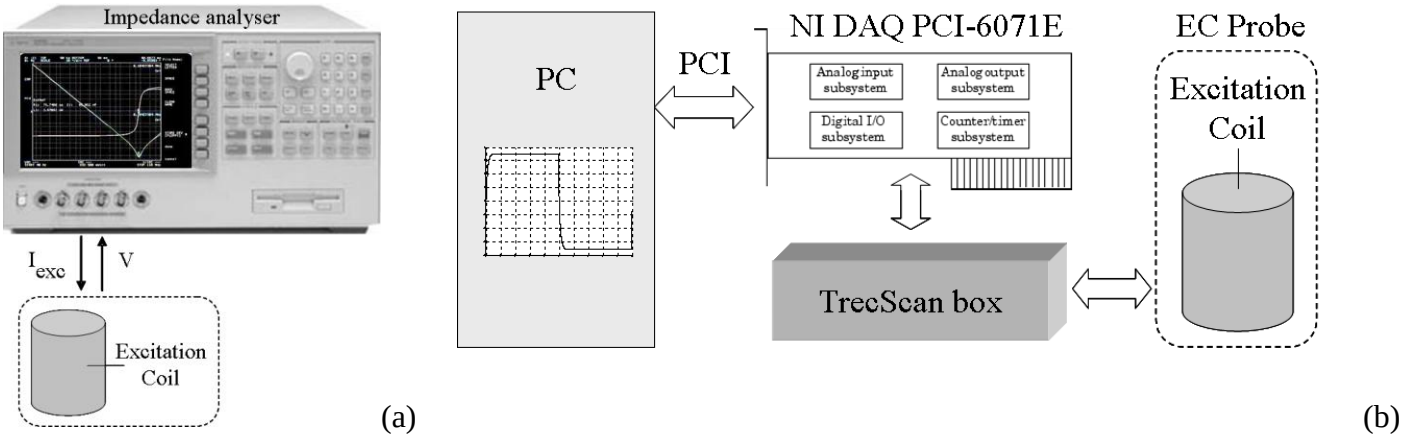

Figure 3. Experimental setup: (a) SFEC and (b) PEC.

The QinetiQ 'TMF' model PEC probe [2] was used in the measurements both by SFEC and PEC techniques. An Agilent 4294A impedance analyzer was used for SFEC measurements as shown in Fig.3-a (application of such a system for EC conductivity spectroscopy was reported in [6]). The operational mode was the following: harmonic signals in current excitation mode Iexc = 20 mA swept in frequency range from 40 Hz to 100 kHz. The EC response was readout from the impedance analyzer as the excitation coil series resistance and inductive reactance depending on frequency.

The QinetiQ TRECSCAN® system was used for PEC measurements. The PEC setup is shown in Fig.3-b. TRECSCAN® operates in current excitation mode with an exponentially damped square wave of duty cycle 50%. The selected period was 10 ms and amplitude Iexc = 250 mA. The PEC response was measured as an impedance change given as a ratio of the induced voltage on the excitation coil and the excitation current.

Both the voltage and the excitation current were acquired as 100 periods of the respective waveforms with sampling rate of 250 kS/s.

3. Results and discussion

3.1 SFEC

Fig.4 shows SFEC responses to steps of various thicknesses (sample no. 1) obtained with the impedance analyzer. The responses are represented as the real (resistance) δR and imaginary (reactance) δXL parts of the coil impedance change due to eddy currents normalized to the absolute value of the coil impedance measured on the thickest (10 mm) sample:

$$\delta R_{step} = (R_{step} - R_{10mm}) / abs(Z_{10mm}) * 100\%; \quad (2)$$

$$\delta X_{L\,step} = (X_{L\,step} - X_{L\,10mm}) / abs(Z_{10mm}) * 100\%. \quad (3)$$

The responses from sample no. 1 offer unambiguous thickness quantification based on the magnitude and position of the spectral peak. The frequency at the peak response increases with decreasing sample thickness, which follows from the depth of penetration relationship (1) [5].

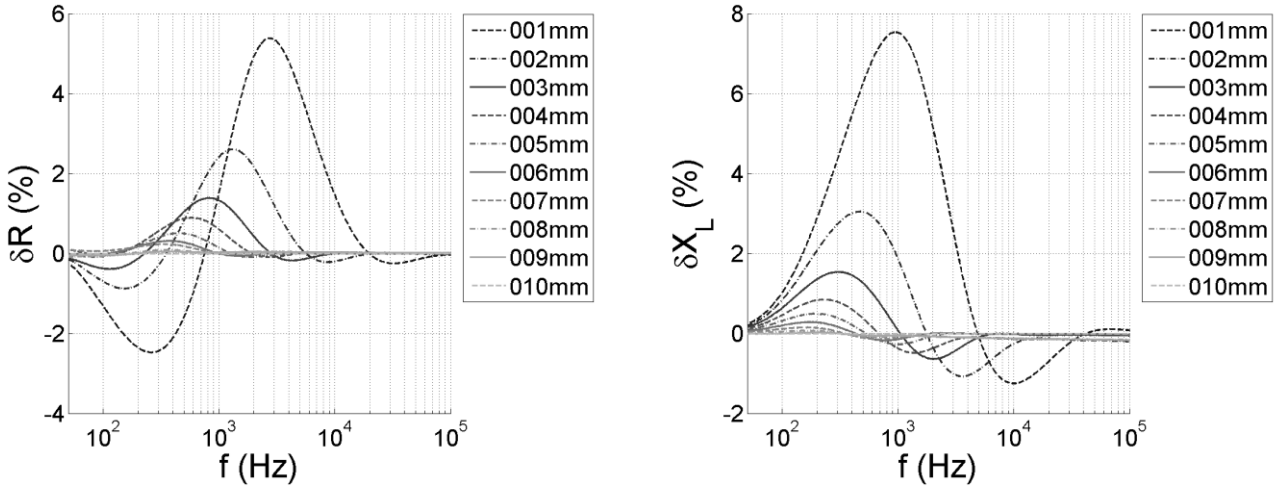

(a) (b)

Figure 4. Normalised SFEC response to sample no.1 with steps of various thickness: (a) real and (b) imaginary components.

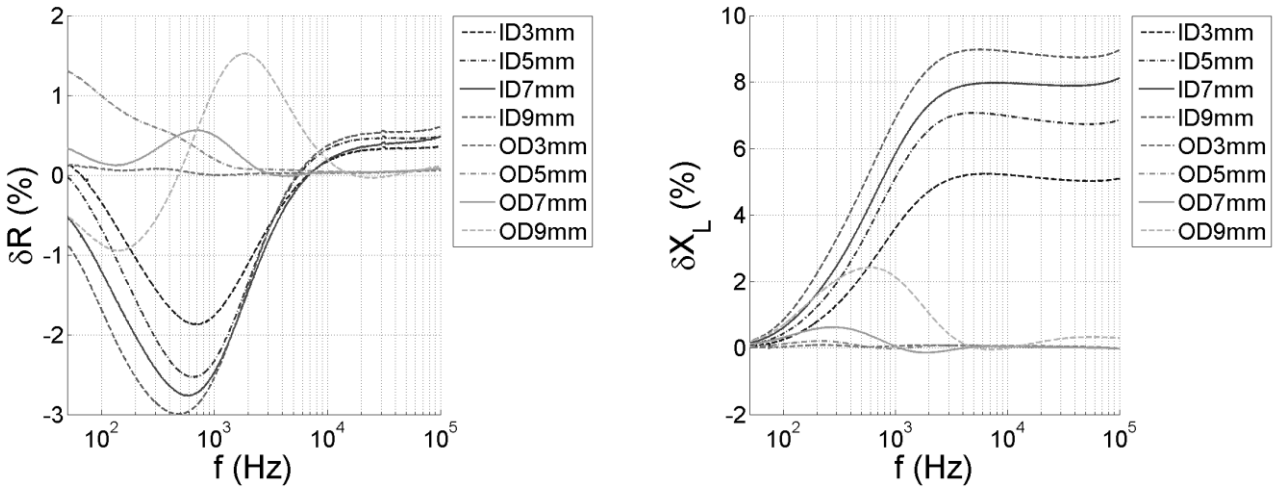

(a) (b)

Figure 5. Normalised SFEC response to sample no.2 with various slots: (a) real and (b) imaginary components.

Fig.5 shows SFEC responses to slots of various depths (sample no.2) obtained with the impedance analyzer. The responses are represented as the real (resistance) and imaginary (inductance) parts of the coil impedance change due to eddy currents normalized to the absolute value of the coil impedance measured on a free of defect segment of the sample:

$$\delta R_{slot} = (R_{def} - R_{no\text{-}def}) / abs(Z_{no\text{-}def}) * 100\%; \quad (4)$$

$$\delta X_{L\ slot} = (X_{L\ def} - X_{L\ no\text{-}def}) / abs(Z_{no\text{-}def}) * 100\%. \quad (5)$$

The responses from sample no. 2 offer unambiguous discrimination between type of slot (ID or OD) based on the signal pattern, since OD slots have no high frequency response due to the skin effect. It is worthwhile noting that the responses to OD slots exhibit similar dependence on the slot depth as the previous responses dependence on the varying sample thickness (compare to Fig.4) and that the similarity is limited by the slot width. The responses also enable slot depth quantification based on the signal magnitude.

3.2 PEC

Fig.6-a shows one half-period of the PEC excitation current waveform. In order to represent PEC signals in the frequency domain the Discrete Fourier Transform (DFT) was performed. Due to the high sampling rate (250 kS/s) and large number of samples (250 k samples) the spectral resolution achieved was 1 Hz. Signals in the frequency domain were decimated in order to contain only the fundamental frequency and its odd harmonics since a square waveform contains odd harmonics of the repetition frequency whose amplitudes decay inversely to the number of harmonic n:

$$f(t) = \frac{4}{\pi} \sum_{n=1,3...}^{\infty} \frac{1}{n} \sin(n\omega_0 t) \quad (6)$$

where ω_0 is the angular frequency of repetition. The other frequency components are essentially zero. Fig.6-b shows the spectrum of the excitation current.

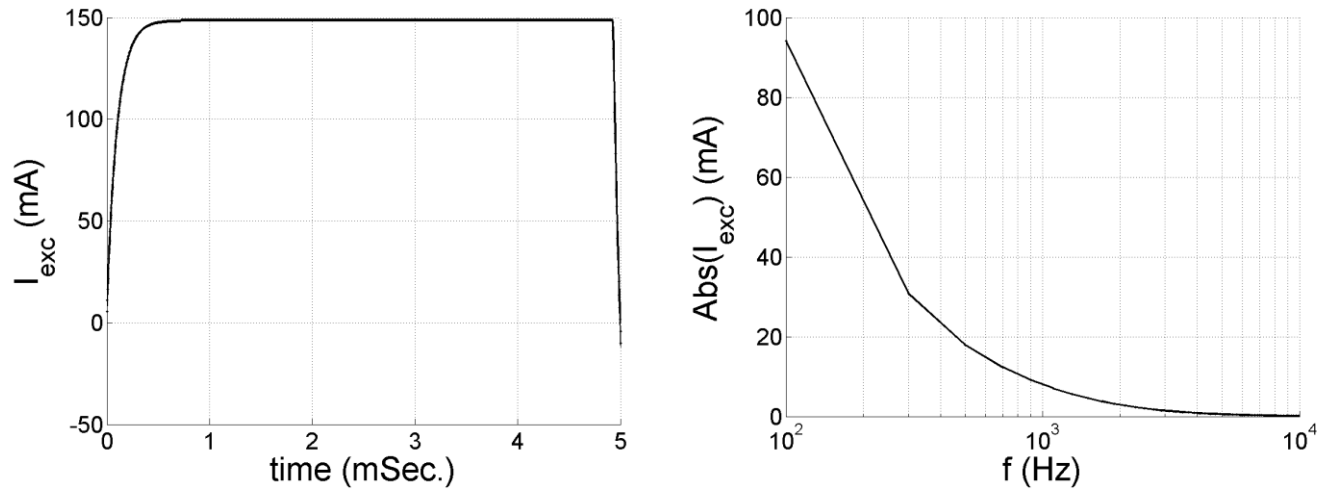

(a) (b)

Figure 6. Excitation current of PEC: (a) waveform; (b) frequency domain.

Fig.7-a shows one quarter-period of the total PEC voltage waveform due to steps of various thicknesses (sample no. 1). The complete waveform period consists of a positive pulse followed by an identical negative pulse. Fig.7-b shows one half-period of the respective difference PEC voltage waveform obtained by subtracting the signal measured on the reference thickness (10 mm) segment of the sample (denoted as background) from the total signals. The time domain difference responses offer thickness quantification based on the peak position and the peak magnitude. The delay to the peak position increases with increasing thickness due to longer diffusion times of eddy currents into the material. The peak magnitude decreases and eventually vanishes as the step thickness approaches the reference thickness (10 mm).

In order to compare the PEC response with SFEC measurements, the respective impedance change was calculated as the ratio of the voltage induced across the excitation coil and the controlled excitation current driven through the coil: $\delta Z(f) = \delta V(f)/I_{exc}(f)$.

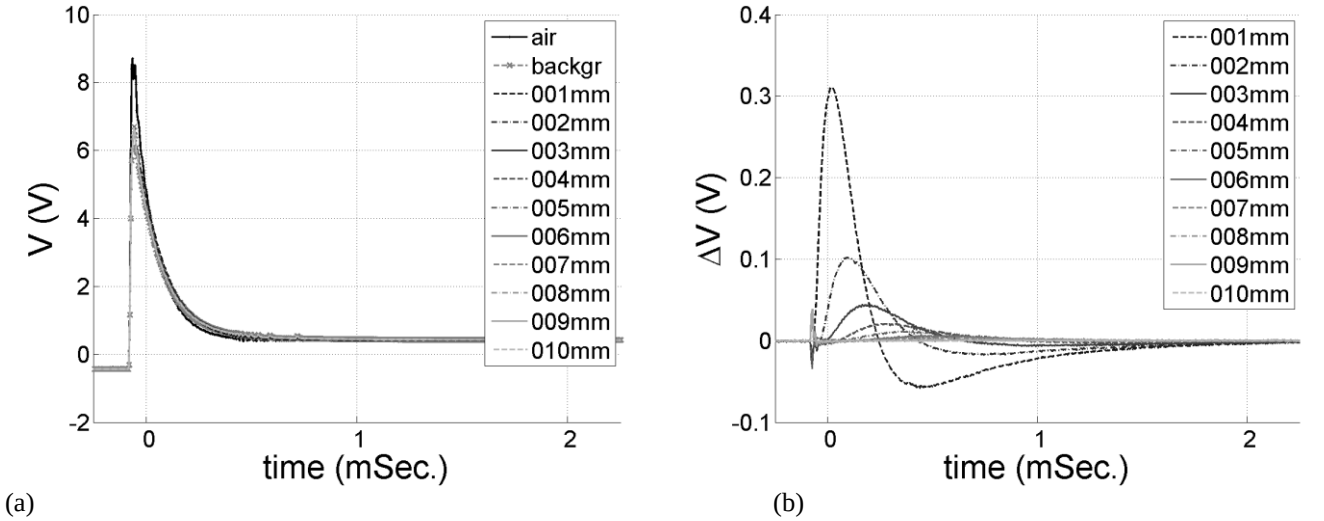

(a) (b)

Figure 7. Time domain PEC response to sample no.1 with steps of various thickness: (a) total and (b) difference signal. Background signal corresponds to the free of defect part of the sample. One quarter-period of the repetitive response signal is shown.

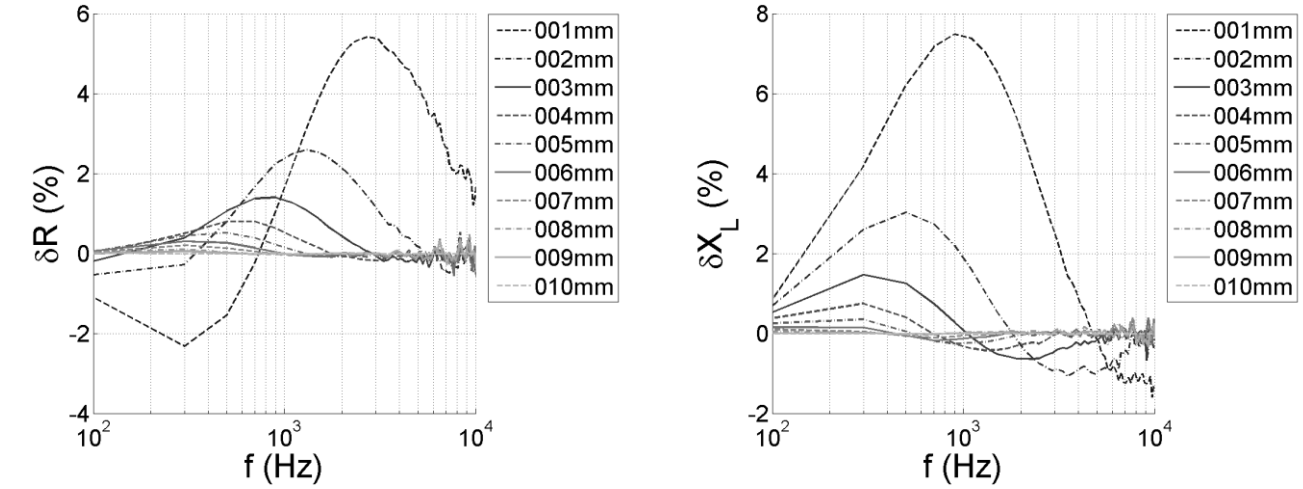

(a) (b)

Figure 8. Normalised spectral PEC response to sample no.1 with steps of various thickness: (a) real and (b) imaginary components.

Fig.8 shows spectral PEC responses to steps of various thicknesses (sample no. 1). The responses are represented as the real (resistance) and imaginary (inductance) parts of the coil impedance change due to eddy currents normalized to the absolute value of the coil impedance measured on the thickest (10 mm) sample according to expressions (2) and (3). The PEC method shows excellent quantitative agreement with the SFEC responses. The high frequency components in Fig. 8 have poor signal-to-noise ratio due to low amplitude of the high frequency components of the excitation current waveform. Two reasons for the low amplitude of the high frequency components are:

- the square waveform contains odd harmonics of the repetition frequency whose amplitude decays inversely to the number of harmonic (see Fig. 6-b and expression (6));
- the actual excitation signal is an exponentially damped step function with time constant of 100 μs;
- the excitation circuit contains a low-pass filter with cut-off frequency 10 kHz.

For the SFEC responses a constant current method was used in the impedance analyser. Although this maintains a constant magnetic field across the band of frequencies the eddy-current density will increase with frequency. In the PEC case, the reduction in the amplitude of the high frequency content is offset by the increase in eddy-current density with frequency and the spectrum of the initial eddy-current pulse tends towards uniform amplitude across the band.

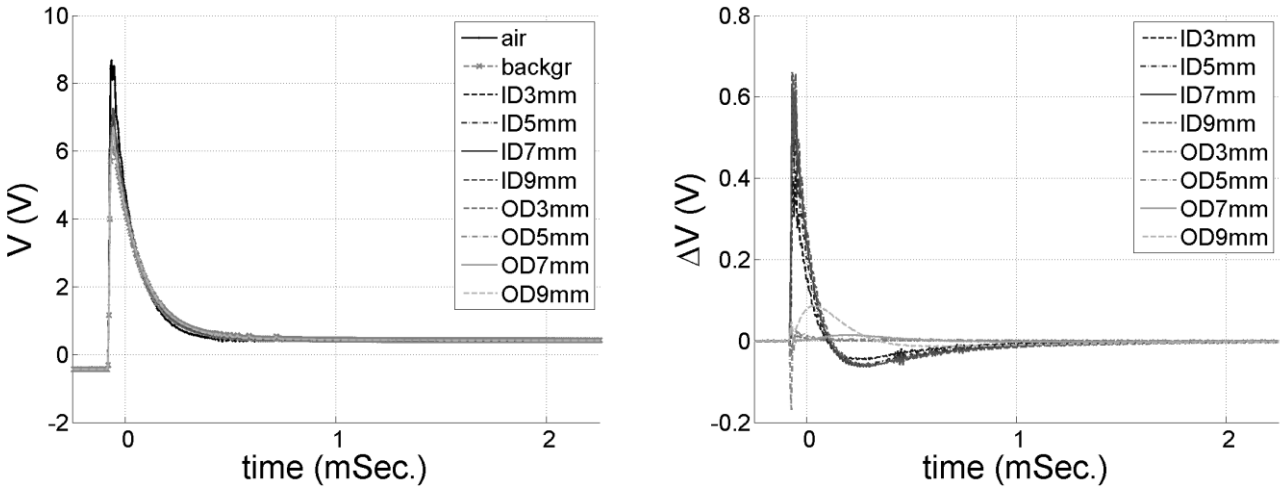

(a) (b)

Figure 9. Time domain PEC response to sample no.2 with various slots: (a) total and (b) difference signal. Background signal corresponds to the defect-free part of the sample. One quarter-period of the repetitive response signal is shown.

Fig.9-a shows one quarter-period of the total PEC voltage waveform due to various slots (sample no. 2). The complete waveform period consists of a positive pulse followed by a identical negative pulse. Fig.9-b shows one half-period of the respective difference PEC voltage waveform obtained by subtracting the signal measured on a free of defect segment of the sample (denoted as background) from the total signals. The time domain difference responses enables discrimination between various slots based on peak position and peak magnitude.

Fig.10 shows spectral PEC responses to various slots (sample no. 2). The responses are represented as the real (resistance) and imaginary (inductance) parts of the coil impedance change due to eddy currents scattered by slots normalized to the absolute value of the coil impedance measured on the defect free segment of the sample (background signal) according to expressions (4) and (5). Again the PEC signals show excellent quantitative agreement with the SFEC responses at low frequencies.

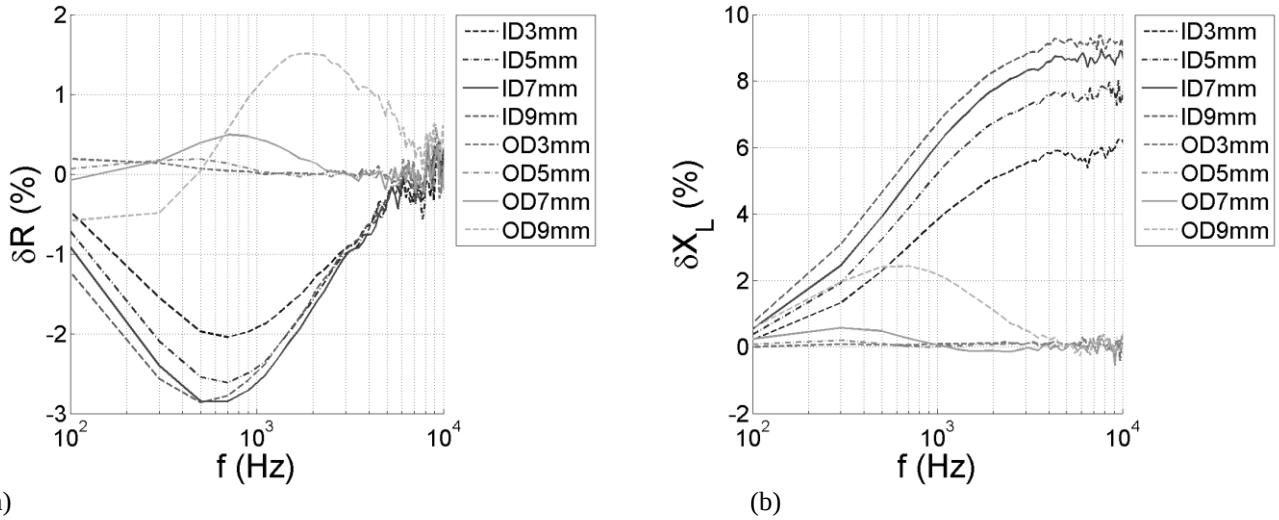

(a) (b)

Figure 10. Normalised spectral PEC response to sample no.2 with various slots: (a) real and (b) imaginary components.

4. Conclusions

Even though remarkable results obtained with PEC on thick structures have been reported in numerous publications, the present work clearly demonstrates and offers an explanation of the advantages of PEC over traditional swept and multi-frequency techniques at low inspection frequencies up to 10 kHz. While both methods (SFEC and PEC) provide reliable discrimination of the upper and lower (reverse) surface slots as well as among various sample thickness, using PEC we can obtain comparable quantitative information in a single excitation cycle. For both PEC and SFEC the response to OD slots exhibit similar dependence on the slot depth as the responses to varying sample thickness since the changing slot depth equates to different thickness of material above the slot, although the width of the slot limits the similarity.

Future work needs to: 1) determine suitable parameters or features for quantitative characterisation of various test cases, 2) build frequency domain relationships between PEC impedance measurement and PEC response obtained with a magnetic field sensor and determine their implication for the time domain signal interpretation and 3) investigate the potential for increasing the high frequency excitation for PEC systems by applying an appropriate excitation waveform and the benefits that this increase may provide.

Acknowledgement

This work was funded by an EPSRC grant [EP/E005071/1]. The authors would like to express gratitude to QinetiQ Ltd. for providing the TRECSCAN® PEC system for the study.
TRECSCAN is a Registered Trademark of QinetiQ Ltd.

References

[1] D. J. Harrison, *Characterisation of cylindrical eddy-current probes in terms of their spatial frequency spectra*, Science, Measurement and Technology, IEE Proc., Vol. 148, No. 4 (2001) 183-186

[2] R. A. Smith, D. Edgar, J. Skramstad and J. Buckley, *Enhanced transient eddy current detection of deep corrosion*, Insight – NDT and condition monitoring, Vol. 46, No. 2 (2004) 88-91

[3] X. Ma, A. J. Peyton and Y. Y. Zhao, *Measurement of the electrical conductivity of open-celled aluminium foam using non-contact eddy current techniques*, NDT&E Int., Vol. 38, No. 5 (2005) 359-367

[4] X. Ma, A. J. Peyton and Y. Y. Zhao, *Eddy current measurements of electrical conductivity and magnetic permeability of porous metals*, NDT&E Int., Vol. 39, No. 7 (2006) 562-568

[5] W. Yin and A. J. Peyton, *Thickness measurement of non-magnetic plates using multi-frequency eddy current sensors*, NDT&E Int., Vol. 40, No. 1 (2007) 43-48

[6] B. A. Abu-Nabah, P. B. Nagy, *High-frequency eddy current conductivity spectroscopy for residual stress profiling in surface-treated nickel-base superalloys*, NDT&E Int., Vol. 40 (2007) 405–418

[7] F. Thollon, B. Lebrun, N. Burais and Y. Jayet, *Numerical and experimental study of eddy current probes in N DT of structures with deep flaws*, NDT&E Int., Vol. 28, No. 2 (1995) 97-102

[8] B. Benoist, P. Gaillard, M. Pigeon and P. Morizet-Mahoudeau, *Expert system for the characterization of defect signals in steam generator tubes*, Eng. Applications of Artificial Intelligence, Vol. 8, No. 3 (1995) 309-318

[9] S. K. Burke, G. R. Hugo, and D. J. Harrison, *Transient eddy-current NDE for hidden corrosion in multilayer structures*, Rev. Prog. in QNDE, Vol. 17A (1998) 307-314

[10] G. Y. Tian and A. Sophian, *Defect classification using a new feature for pulsed eddy current sensors*, NDT&E Int., Vol. 38, No.1 (2005) 77-82

[11] B. Lebrun, Y. Jayet and J. C. Baboux, *Pulsed eddy current signal analysis: application to the*

experimental detection and characterization of deep flaws in highly conductive materials, NDT&E Int., Vol. 30, No. 3 (1997) 163-170

[12] A. Sophian, G. Y. Tian, D. Taylor and J. Rudlin, *A feature extraction technique based on principal component analysis for pulsed Eddy current NDT*, NDT&E Int., Vol. 36, No. 1 (2003) 37-41

[13] T. Clauzon, F. Thollon, A. Nicolas, *Flaws Characterization with Pulsed Eddy Currents N.D.T.,* IEEE Trans. Mag., Vol. 35, No. 3 (1999) 1873-1876

[14] Toshihiko Kiwa, Tomoaki Kawata, Hironobu Yamada and Keiji Tsukada, *Fourier-transformed eddy current technique to visualize cross-sections of conductive materials*, NDT&E Int., Vol. 40, No. 5 (2007) 363-367